Journal Name

ARTICLE TYPE

Cite this: DOI: 10.1039/xxxxxxxxxx

Aminophenol isomers unraveled by conformer-specific far-IR action spectroscopy†

Vasyl Yatsyna,[a,b] Daniël J. Bakker,[b] Raimund Feifel,[a] Anouk M. Rijs,*[b] and Vitali Zhaunerchyk*[a]

Received Date
Accepted Date

DOI: 10.1039/xxxxxxxxxx

www.rsc.org/journalname

Spectroscopic studies of molecular structure can strongly benefit from extending the conventional mid-IR range to the far-IR and THz regions, as low-frequency molecular vibrations provide unique fingerprints and high sensitivity to intra- and intermolecular interactions. In this work, the gas-phase conformer specific far-IR spectra of aminophenol isomers, recorded in the spectral range of 220-800 cm^{-1} at the free-electron laser laboratory FELIX in Nijmegen (the Netherlands), are reported. Many distinct far-IR vibrational signatures which are specific for the molecular structure of the different aminophenol isomers are revealed and assigned. The observed far-IR transitions of the NH_2 wagging (inversion) motion have been treated with a double-minimum harmonic well potential model that has enabled us to obtain the inversion barrier values. Moreover, we discuss the limitations and capability of conventional DFT frequency calculations to describe the far-IR vibrational modes.

1 Introduction

Far-infrared (IR) and TeraHertz (THz) photons excite low-frequency molecular vibrations and spectroscopy in these spectral regions provides an opportunity for studying molecular systems of biological importance. As far-IR and THz spectra yield unique fingerprints of molecular structure and are highly sensitive to intra- and intermolecular interactions [1–4], spectroscopy in this spectral region has great potential to elucidate the structure of protein conformations as well as to study how the functions of different conformations are affected by intra- and intermolecular interactions. In particular, the elucidation of conformational structure is crucial for resolving many biological and medical challenging issues, such as misfolding and aggregation of proteins associated with neurodegenerative diseases [5,6].

The research field employing low-frequency vibrations in biomolecular systems evolved significantly since the first far-IR studies of small biomolecules, peptides and proteins in the early 1970s [7,8], to more complex investigations of a wide variety of biomolecules with the advance of THz technology in the early 1990s. Previous studies in the THz region were mainly focused on conformational changes in proteins, intermolecular interactions such as ligand binding, the protein hydration layer and its dynamics [9], as well as structural information [1,3,4,10,11] which complements the data obtained from the well-established mid-IR vibrational spectroscopy technique [12].

So far the widespread application of THz and far-IR spectroscopy in structural studies is hindered by several difficulties, such as the low absorption cross-section and unreliable theoretical predictions. The latter is due to the fact that low-frequency vibrations are highly non-local and anharmonic. In this respect, gas-phase studies of molecular vibrations have several advantages compared to the condensed phase, as they enable a direct comparison with computer simulations performed on isolated systems. Additionally, they directly reflect the intrinsic properties of the molecules without the influence of interactions with the surrounding solvent or crystalline matrix. After gaining a profound understanding of vibrational signatures of gas-phase biomolecules, this knowledge can be applied for the analysis of more complicated spectra obtained in natural environments. Gas-phase mid-IR spectroscopy combined with theoretical calculations was demonstrated to be successful in the structural analysis of molecules of biological interest [12], even up to systems as large as the pentadecapeptide gramicidin [13] and decapeptide Gramicidin S [14–17]. However, due to the high density of vibrational states, the mid-IR spectra are often congested, so that they

[a] University of Gothenburg, Department of Physics, 412 96 Gotheburg, Sweden. Tel: +46317869150; E-mail: vitali.zhaunerchyk@physics.gu.se

[b] Radboud University, Institute for Molecules and Materials, FELIX Laboratory, Toernoovield 7-c, 6525 ED Nijmegen, The Netherlands. Tel: +31243653940; E-mail: a.rijs@science.ru.nl

† Electronic Supplementary Information (ESI) available: comparison between experimental and theoretical wavenumbers calculated for the studied isomers of aminophenol with harmonic approximation and VPT2 approach using B3LYP/aug-pc-2 level of theory. See DOI: 10.1039/b000000x/

require the use of additional techniques to resolve individual mid-IR bands, for example, two-dimensional IR spectroscopy[18]. Furthermore, the mid-IR data quite often allow only assignment of families of structures[13]. In these cases the far-IR and THz spectra are expected to be an effective alternative providing structure specific information on biomolecules. Indeed, even for relatively small peptides, dipeptides, it was recently shown that structural information extracted from far-IR signatures is superior to that obtained from mid-IR data[10,11].

Although far-IR and THz spectroscopic studies of molecular conformations are of great significance for biology, only few techniques enable such studies in the gas-phase. Currently, free electron lasers (FELs) offer the unique possibility to study conformational-selective far-IR and THz spectra of gas-phase molecules. In contrast to other existing far-IR and THz sources, FELs are characterized by high spectral brightness in combination with continuous wavelength tunability in a broad range of frequencies, from THz to mid-IR. In the present work we employ FEL based far-IR/UV ion-dip spectroscopy[19] of three aminophenol isomers to measure the lowest frequency vibrational modes and to identify conformer-specific vibrational bands. The molecule aminophenol ($C_6H_4(OH)NH_2$, see Fig. 1) consists of a chromophore (phenyl ring) and two functional groups, namely the hydroxyl OH and the amino NH_2 group. The three positional isomers of aminophenol differ in the location of the NH_2 group with respect to the OH group, and are named as *ortho*- (2-AP), *meta*- (3-AP) and *para*- (4-AP) aminophenol (cf. Fig. 1). In addition, 2-AP and 3-AP exhibit rotational isomerism for different orientations of the OH group relative to the amino group, leading to the distinct *trans* and *cis* conformers. In the case of 2-AP the close proximity of the substituents leads to the formation of NH$\cdots$O or OH$\cdots$N intramolecular hydrogen bonds. As mentioned earlier, some low-frequency vibrational modes are strongly anharmonic and it is a challenge for modern quantum chemical methods to describe these modes. In the present work, we also evaluate the feasibility of DFT frequency calculations to reproduce the far-IR spectra of aminophenol isomers both within the double harmonic approximation and by applying anharmonic second order-vibrational perturbation theory (VPT2)[20–22].

2 Methods

2.1 Experimental details

The experimental work was carried out at the free electron laser laboratory FELIX at the Radboud University in the Netherlands. The far-IR spectra of internally cooled aminophenol were recorded under supersonic jet conditions utilizing IR-UV ion-dip spectroscopy[19]. For this technique the frequency of a table-top UV dye laser is tuned to the electronic transition of the specific molecular species to produce a constant ion signal by resonance-enhanced multi-photon ionization (REMPI). The intensity of the REMPI signal is proportional to the population of the vibrational ground state of the S_0 electronic state. Prior to the irradiation with the UV dye laser, the molecules interact with the tunable IR laser beam provided by the free electron laser FELIX. If the IR photon energy is resonant with a vibrational transition, the

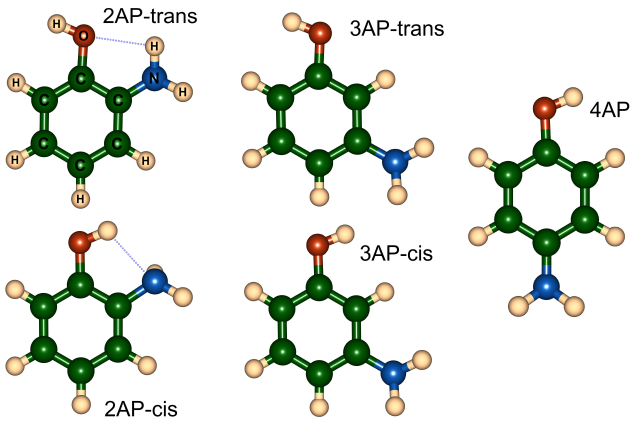

Fig. 1 Optimized geometries of aminophenol isomers, namely 2-AP (*trans* and *cis* conformers), 3-AP (*trans*, *cis*), and 4-AP. The amino (NH_2) group is out of plane with respect to the aromatic ring. Geometry optimization was performed with the B3LYP/aug-cc-pVTZ method.

population of the vibrational ground state is depleted, and hence the intensity of the REMPI signal is reduced. By tuning the IR laser wavelength and monitoring the ion signal, ion-dip spectra are recorded, in which the dips are associated with excitations of vibrational transitions.

A heatable molecular beam source was used to deliver the sample species to the interaction region. The crucible of the oven was filled with aminophenol powder of a particular isomeric configuration and was resistively heated to 80-90 °C which provided a sufficient amount of target molecules in the interaction volume. Three different isomeric forms of aminophenol were obtained commercially (Sigma Aldrich) with a stated purity >99 %. Helium at high pressure (3 bar) was used as a carrier gas to create a supersonic flow enabling efficient cooling of the internal degrees of freedom of the molecules. The parent ions, created using a (1+1)-REMPI scheme, were monitored with a time-of-flight mass spectrometer. During IR-UV ion-dip measurements the wavelength of the UV dye laser was selected to correspond to the REMPI transition of either the *trans* or the *cis* conformer. FELIX was operated at 5 Hz delivering few μs long pulses with wavelength-dependent energy ranging from 15 to 35 mJ. The UV laser was operated at a rate of 10 Hz providing reference measurements of the ion signal without FELIX irradiation at every second pulse (10/5 Hz scheme). The far-IR spectra were measured in the wavelength range of 220-800 cm^{-1} (12-45 μm) with a bandwidth (FWHM) of FELIX about 1 %.

2.2 Computational details

Both the structure optimization and the vibrational frequency calculations were performed using the Gaussian 09 package[23]. Stable structures of all aminophenol isomers and their corresponding conformers (*cis* and *trans*) were obtained as a stationary point of the potential energy surface by applying a geometry optimization procedure with different combinations of DFT functionals and basis sets. The optimized geometries were then used in the calculations of the harmonic vibrational frequencies at the same level

of theory. The anharmonic vibrational frequencies were calculated using a generalized second order vibrational perturbation theory (VPT2) as implemented in the Gaussian package[21,22]. In all optimizations and frequency calculations we used the "*Tight*" convergence criterion for optimization, an "*Ultrafine*" (99,590) integration grid for the evaluation of two-electron integrals and a "*Fine*" (75,302) grid for coupled perturbed Kohn-Sham (CPKS) computations. This was done in order to increase the accuracy of the harmonic and anharmonic calculations as suggested by Barone *et al.*[21] A more coarse grid was used for the CPKS computations to efficiently reduce the computational cost, as tests with larger (99,590) grid produced almost identical harmonic and anharmonic frequencies. The evaluation of the influence of the basis set on the accuracy of far-IR frequencies calculated with VPT2 was performed with B3LYP functional[24], which was shown to be reliable for the medium-sized semi-rigid molecules[22].

The potential energy profile governing the NH_2 wagging (inversion) motion was calculated by means of a relaxed potential energy scan at the B3LYP/cc-pVTZ level with the Gaussian 09 software. The angle between the plane of the amino group and the phenyl ring was fixed, while the HNH angle and all bond distances were relaxed during the optimization procedure. The changes in HNH angle and r_{N-H} distances were taken into account when fitting the calculated potential to the a double-minimum harmonic well potential with a Gaussian barrier[25]. The corresponding reduced mass of 1.93 a.m.u. for NH_2 inversion motion of aminophenol was used. The B3LYP/cc-pVTZ level of theory was chosen for the calculations, because the barriers to NH_2 inversion estimated with second-order Møller-Plesset (MP2/cc-pVTZ) method were much higher than the barriers obtained from experiment. It is worth to note that for aniline the Hartree-Fock and MP2 calculations with small double-zeta basis sets[26] provided good agreement between experimental values of the barrier and *ab initio* results. However, the agreement was considered rather fortuitous, and we decided not to use these approaches in this study.

As the vibrational modes in the far-IR range studied are highly non-local, we used the method of potential energy distribution (PED) analysis to quantitatively describe the contribution of a given group of atoms to a particular normal mode. The PED analysis was performed employing the VEDA4 program[27].

3 Results

3.1 REMPI spectra

The REMPI spectra recorded for all aminophenol isomers are presented in Fig. 2. The observed REMPI transitions are in good agreement with previously published data[28–30]. In the case of 2-AP, the most intense peaks are associated with the *trans* conformer, with the origin at 33459.5 cm^{-1}. It is worth mentioning that the intensity of the origin peak of 2-AP is lower compared with the vibrational progression transitions, which might be an indication of a strong change in geometry of the exited state involved in REMPI[28]. No evidence of transitions corresponding to the *cis* conformer of 2-AP were found in the UV frequency range of 33350-34350 cm^{-1} under the supersonic jet expansion conditions with He or Ar as the carrier gas. This result is consistent with previous studies[28,31], where it was shown that under these conditions the *trans* conformer is more favorable than the *cis*. A possible reason is a strong resonance stabilization of the *trans* conformer due to the donation of electron density from the NH_2 group to the aromatic ring. The resonance is altered upon rotation of the NH_2 group and the loss of stabilization is not compensated by the formation of the OH···N hydrogen bond in the case of the *cis* conformer[31].

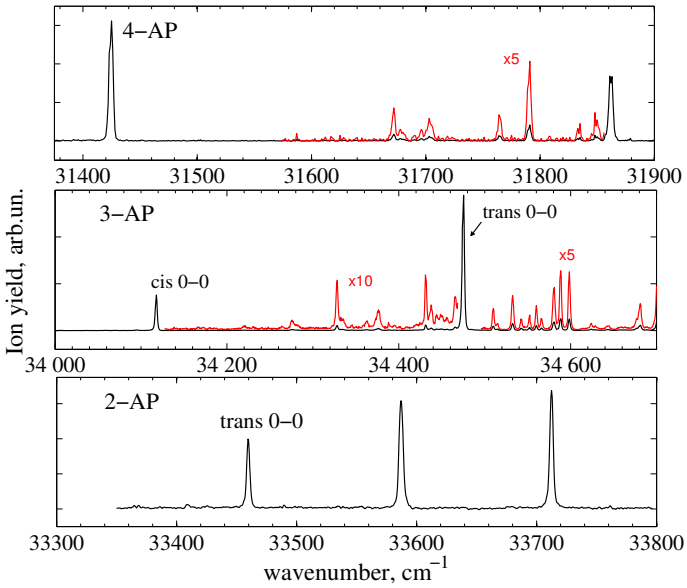

Fig. 2 (1+1)-REMPI spectra of aminophenol isomers in the vicinity of the 0-0 origin. The origins of the *cis* and the *trans* conformer(s) are denoted as "*cis* 0-0" and "*trans* 0-0", respectively. The assignment of the origin transitions have been adopted from Refs.[28,29] and were verified in the present experiment by measuring IR spectra with the UV laser tuned to these transitions.

3.2 Experimental far-IR ion-dip spectra and assignment

Fig. 3 shows experimental far-IR absorption spectra of the aminophenol isomers/conformers in the range of 220-800 cm^{-1}, averaged over several IR-UV ion-dip scans. The spectra were corrected for the wavelength-dependent number of far-IR photons of FELIX pulses. The average linewidth of the vibrational peaks is close to 1 %. As one can see, the far-IR spectra of different isomers show plenty of distinct absorption bands, which have different positions and intensities for each isomeric form. Moreover, two conformers of 3-AP are also well resolved in this range, despite the fact that they differ only in the orientation of the hydroxyl group. Indeed, the non-local character of the vibrations in the far-IR range influences the strong structural dependence of the observed far-IR spectra, even in the case when the difference in structure is minor. DFT calculations of force constants and the frequency analysis, performed within the harmonic approximation, predict a considerably lower number of fundamental transitions (normal modes) than the number of observed experimental bands in this range. This fact indicates that a number of overtones and combination bands is present in the measured spectra

complicating the full vibrational assignment. Nevertheless, we were able to assign the majority of the bands with the help of data from literature for similar molecules (such as disubstituted benzene derivatives[32], aniline and halosubstituted anilines[33,34]). The assignments were supported where possible with more accurate frequency calculations based on the anharmonic VPT2 treatment[22]. The results of our theoretical B3LYP/aug-pc-2 calculations are collected in the ESI†. In what follows, we will discuss the isomer selectivities and similarities of the observed vibrational transitions of aminophenol.

The characteristic fundamental bands which correspond to phenyl ring deformations and bending vibrations of substituent OH and NH_2 groups are outlined and marked with different colors in Fig. 3. Among different isomers there are substantial variations in the position of all ring deformation bands, either in plane (i.p., CCC bending) or out of plane (o.p., CCCC torsion). For instance, the strongest ring o.p. band, **16b** according to Varsanyi's notation[32], is observed at 502 cm^{-1} for 4-AP, while in the case of *trans* 2-AP it is shifted to 445.5 cm^{-1} (see Fig. 3(a)). The observed frequencies of another two ring o.p. vibrations, **16a** and **4**, are 422 and 676.5 cm^{-1} for 4-AP, and in the case of *trans* 2-AP they are significantly higher, namely 501 cm^{-1} and 748.5 cm^{-1}. Ring i.p. bands **6a** and **6b** are less intense, and are observed as two separate peaks at 486 and 542 cm^{-1} in the case of *trans* 2-AP, while there is no clear evidence of these bands for 4-AP. We note that the weak band at 542 cm^{-1} of 2-AP was reproducible in a series of measurements which implies that this feature is unlikely to be due to noise. In the case of 3-AP, **6a** and **6b** were observed as two closely lying bands around 430 cm^{-1} (see Fig. 3(b)), slightly red-shifted in the spectrum of the *trans* conformer with respect to the *cis*. According to the DFT frequency calculations, the C-O o.p. bending mode **10b** of 4-AP should appear at $\approx$ 350 cm^{-1} and the experimental spectrum indeed shows a peak at this frequency. However, due to the relatively low intensity of this peak, we cannot rule out an alternative assignment where the **10b** C-O o.p. bending mode overlaps with the C-O i.p. bending fundamental at 370 cm^{-1} (**9b**). This assertion is supported by a relatively broad width of the experimental band at 370 cm^{-1} compared with others.

Another important set of far-IR bands corresponds to torsional vibrations of the OH and NH_2 functional groups. The frequencies of these vibrations are highly influenced by the form of the torsional potential energy profile and the value of barrier to internal rotation. The NH_2 torsion mode is observed as a relatively strong band at 237 cm^{-1} for 4-AP, at 329 and 318.5 cm^{-1} for the *trans* and *cis* conformers of 3-AP, respectively, and at 323 cm^{-1} for *trans* 2-AP. The OH torsion mode shows a strong absorption band at 254.5 cm^{-1} for 4-AP, 316 and 307 cm^{-1} for the *trans* and *cis* conformers of 3-AP, respectively, and 286.5 cm^{-1} for *trans* 2-AP. In the case of 2-AP, we also observe a so called hydrogen bond stretching mode at 303 cm^{-1} involving the motion of the atoms of the amino and hydroxyl groups towards each other (C-O, C-N i.p. bending mode).

The studied spectra of aminophenol also contain the transitions corresponding to the NH_2 wagging (inversion) mode, similarly to the aniline-like molecules[33,34]. This vibration involves the out

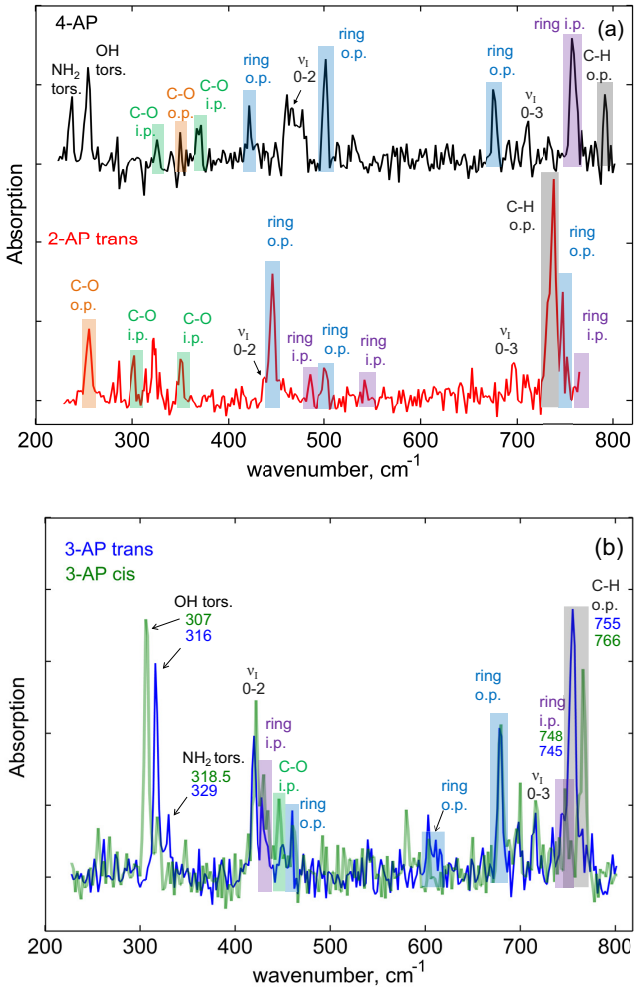

Fig. 3 Experimental absorption spectra of 4-AP and *trans* 2-AP (a) and *trans* and *cis* 3-AP (b) in the range of 220-800 cm^{-1}, together with the assignments of fundamental vibrational transitions. The ring o.p. transitions are marked in blue, ring i.p. - in pink, C-H o.p. wagging - in grey, C-O i.p. - in green, and C-O o.p. are in orange. The vibrational transitions of the NH_2 inversion mode are denoted as ν_I (0-2 and 0-3).

of plane wagging movement of the two amino hydrogens, which effectively changes the dihedral angle between phenyl ring and amino-group. As the amino-group in aniline and aminophenol are non-planar in the electronic ground state, there is a certain barrier to amino inversion (planarity). In aniline-like molecules the amino-inversion vibration is well known to be strongly anharmonic (large amplitude vibration), due to a double well potential energy curve governing this motion. A relatively small inversion barrier (around 526 cm^{-1} for aniline) results in large inversion (tunneling) splittings of the vibrational energy levels. For instance, the two lowest amino inversion energy levels of aniline correspond to a tunneling doublet of the vibrational ground state with a separation of the levels of 41 cm^{-1}. Detailed far-IR studies on the NH_2 inversion bands of the electronic ground state were reported for aniline and deuterated and halosubstituted (fluoro-, chloro- and bromo-) anilines, where a complete assignment of

Table 1 Observed energy levels of the NH_2 inversion (wagging) and NH_2 torsion motions of aminophenol isomers compared with literature data for *meta*-halosubsituted anilines[33]. Fundamental 0-1 transitions of NH_2 inversion for 3-AP were estimated from tentatively assigned combinational bands with frequencies equal to the sum and difference of the NH_2 torsion fundamental ν_τ and NH_2 inversion fundamentals ν_I, denoted as $\nu_\tau - \nu_I$ and $\nu_\tau + \nu_I$. All energy levels are presented in cm^{-1} with respect to the zero level (0 cm^{-1}).

	NH_2 inversion, ν_I			NH_2 torsion, ν_τ		
Level	1	2	3	ν_τ	$\nu_\tau - \nu_I$	$\nu_\tau + \nu_I$
4-AP	-	467	711	237	-	-
trans 2-AP	-	437	696	323	-	-
trans 3-AP	55 ± 1	420	714	329	274	385
cis 3-AP	50 ± 1	422	717	318.5	268	-
aniline	40.8	423.8	700.1	277	236	305
3-fluoroaniline	52.8	417.6	719.4	291	238	332
3-chloroaniline	53.4	416.4	716.9	289	236	335
3-bromoaniline	54	418.1	717.6	289	235	328

the transitions based on the lowest 4 vibrational levels of the NH_2 inversion mode was made[33,34]. In particular, for aniline it was shown experimentally that the $\nu_1 - \nu_3$ levels lie 41, 424 and 700 cm^{-1} above the zero level, respectively, and the corresponding vibrational transitions 0-1, 0-2, 1-2, 1-3 and 2-3 were observed and assigned.

In the experimental spectra of aminophenol we observe 0-2 and 0-3 vibrational transitions of NH_2 inversion as well. For 4-AP, we assigned the relatively strong band at 467 cm^{-1} to the 0-2 transition (see Fig. 3(a) and Table 1), which is in agreement with the dispersed fluorescence spectra of 4-AP[35] and para-alkoxianilines[36]. The band at 711 cm^{-1} was assigned to the 0-3 transition. In the proximity of this band (see Fig. 3), there are several other weak peaks, which were not well reproduced in several IR scans, and hence were not considered as reliable candidates of this transition. In the case of trans 2-AP, we assigned two bands at 437 and 696 cm^{-1} to the 0-2 and 0-3 transitions of the NH_2 inversion, respectively. For the *trans* and *cis* conformations of 3-AP, we observed the 0-2 transitions at 420 and 422 cm^{-1}, while the 0-3 transitions were observed at 714 and 717 cm^{-1}. Alternatively, the 0-3 transitions might be reflected by the bands at 698 and 700 cm^{-1}, though they most likely originate from one of the possible combination bands in this region (e.g. **10a**+**15**) as suggested by VPT2 calculations.

In the case of 3-AP weak combinational bands have been observed with frequencies equal to the sum and difference frequencies of the NH_2 torsion and inversion fundamentals (see Table 1), similar to the case of *meta*-halosubstituted anilines[33]. The difference frequency bands (274 and 268 cm^{-1} for *trans* and *cis* 3-AP, respectively) are weak but reproducible. The sum frequency band was only observed for *trans* 3-AP (385 cm^{-1}). Although its intensity is low compared with the difference frequency bands, its position fits the overall frequency pattern of the combination transitions. With the help of these tentatively assigned bands we have estimated the NH_2 inversion fundamentals to be 55 and 50 ± 1 cm^{-1} for the *trans* and *cis* 3-AP, respectively. Table 1 compares the observed NH_2 wagging and NH_2 torsion transitions of aminophenol and aniline[34], as well as *meta*-substituted anilines studied previously[33]. As one can see, the nature of the substituent in the *meta*-position only slightly affects the observed transitions of the NH_2 wagging mode. In contrast, the frequencies of the NH_2 torsional fundamentals for 3-AP are larger than for other molecules, and have a difference of 10 cm^{-1} between the *trans* and *cis* configurations.

3.3 VPT2 treatment of weakly anharmonic modes

The frequency of vibrational modes with relatively weak anharmonicity can be calculated with high accuracy by means of VPT2 approach[22]. For aminophenol molecules in the studied range of 220-800 cm^{-1}, the strongly anharmonic modes include the NH_2 wagging, OH and NH_2 torsional motions and ring puckering, which are poorly described by the VPT2 treatment. However, the weakly anharmonic modes are satisfactory reproduced by the VPT2 treatment. This includes ring o.p. and i.p. deformations (if not combined with NH_2 wagging), C-O, C-N o.p. bending, and C-H o.p. wagging vibrations. We performed a generalized VPT2 treatment for the studied aminophenol isomers with different DFT functionals and basis sets, and the comparative analysis of the accuracy of the calculated frequencies for the weak anharmonic modes is outlined in Fig. 4. As can be seen from Fig. 4(a), the VPT2 treatment with the double-zeta basis sets 6-31+G(d,p) and N07D[37,38] of moderate quality in combination with the B3LYP hybrid functional yield remarkable accuracy at relatively low computational cost. The root mean square (RMS) error is improved to 7 cm^{-1} with respect to harmonic counterparts with RMS error of 18 cm^{-1}. As an example, the theoretical spectra calculated with B3LYP/aug-pc2 method are compared with the experimental spectra of 4-AP and 2-AP in Fig. 5. Most of the peaks are reproduced reasonably well by the VPT2 treatment, with the exception of some strongly anharmonic vibrations such as NH_2 wagging and ring puckering. The comparison between the different functionals studied (Fig. 4(b)) shows that the most accurate results are provided by hybrid functionals B3LYP, B3PW91, PBE0, and the dispersion corrected B3LYP-D3 functional, which perform almost equally well.

Besides far-IR, we performed the similar comparative analysis in the fingerprint and mid-IR range, 800-4000 cm^{-1}, where the experimental fundamental frequencies are available from several conformer specific mid-IR measurements (mostly in the OH and NH stretching region)[28,40,41] as well as from the NIST Database[42] in the case of 2-AP and 4-AP. The analysis based on 50 unequivocally assigned mid-IR fundamental transitions shows that the hybrid functionals B3LYP, B3PW91, B97-1 and B3LYP-D3 provide very accurate frequencies, similar to far-IR range results. The overall performance of the tested functionals is also in good agreement with other studies on small- to medium-sized molecules[21,22,43,44]. These observations may be related to the importance of the $\approx 20\%$ inclusion of the exact non-local Hartree-Fock exchange, as pointed out in investigations with modified hybrid functionals[45]. Thus, it can be concluded that for the weakly anharmonic vibrations the VPT2 treatment with hybrid functionals such as B3LYP in combination with double-zeta basis sets of moderate quality provide reliable accuracy. Hence, they can be successfully applied for the vibrational and structural assignment

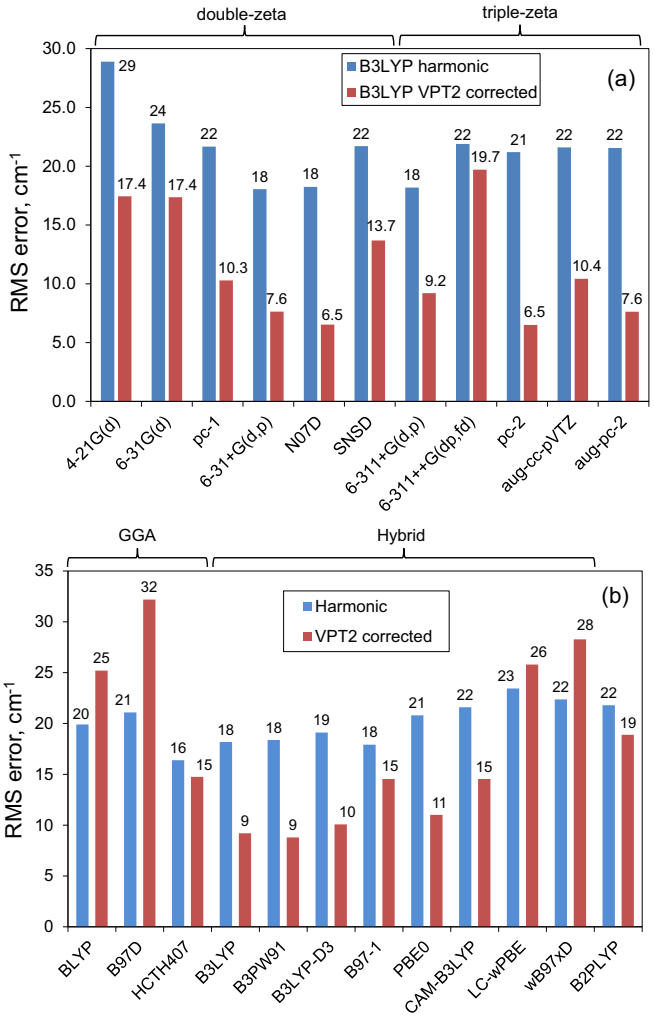

Fig. 4 Comparison between the accuracy of calculated frequencies of weakly anharmonic modes of the aminophenol isomers in the far-IR range of 200-800 cm^{-1}, achieved with different basis sets in combination with the B3LYP hybrid functional (a), as well as achieved with different GGA and hybrid functionals in combination with the 6-311+G(d,p) basis set (b). Results obtained within the harmonic approximation and the anhramonic VPT2 treatment are shown. The root mean square errors are calculated based on 26 observed and assigned fundamentals for all aminophenol isomers in the range of 220-800 cm^{-1}. In the case of the double hybrid B2PLYP functional, the SNSD basis set[38] was used. The EMSL Basis Set Exchange database[39] was used to obtain Jensen's pc-n basis sets, while the N07D basis set was retrieved from Refs.[37,38].

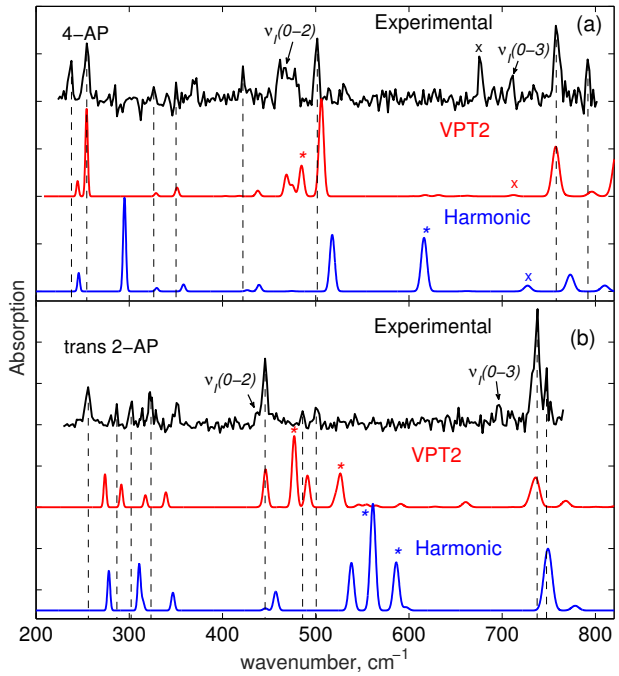

Fig. 5 Comparison between experimental and theoretical spectra of 4-AP (a) and trans 2-AP (b), calculated within harmonic approximation and with VPT2 approach at B3LYP/aug-pc2 level. The theoretical IR peaks associated with NH_2 wagging mode are marked with asterisk (*), while peaks corresponding to ring puckering are marked with cross (x) symbols.

of semi-rigid molecules with a small number of strongly anharmonic vibrations.

3.4 Potential function of NH_2 inversion

In order to describe the strongly anharmonic NH_2 inversion (wagging) motion, we employed a model where the potential energy surface is described by a double-minimum harmonic well with a gaussian barrier[25]. The model was successfully applied previously to explain the far-IR inversion transitions in ammonia, aniline, deuterated and halosubstituted anilines[33,34]. The model potential energy function has the form:

$$V(Q) = \frac{1}{2}\lambda Q^2 + Aexp(-a^2Q^2), \quad (1)$$

where Q is a mass adjusted coordinate defined by $2T = \dot{Q}^2$. As proposed by Coon *et al.*[25], the parameters B, ρ and ν_0 are introduced instead of parameters λ, A and a. In this case $B\nu_0$ denotes the height of the barrier to inversion in cm^{-1}, and ρ and ν_0 are defined by

$$a^2 = e^{\rho}\lambda/2A, \quad (2)$$

$$\lambda = (2\pi c\nu_0)^2. \quad (3)$$

In this notation, ρ determines the relative steepness of the walls of the barrier and the parabolic potential itself, while ν_0 is a harmonic frequency corresponding to parabolic part of the potential. The energy levels for a certain potential function (Eq. 1) are found variationally with a basis set consisting of harmonic oscillator wavefunctions with frequency ν_0.

For *trans* and *cis* conformers of 3-AP, the parameters B, ρ and ν_0 were found by a least squares fitting of the variationally calculated energy levels to the experimental values of 0-1, 0-2 and 0-3 vibrational transitions of NH_2 inversion. The frequencies of the 0-2 and 0-3 transitions were taken from the measured spectra, while the 0-1 transition frequency was calculated from the sum and difference bands with frequencies $\nu_\tau + \nu_I$ and $\nu_\tau - \nu_I$ (see Table 1). The obtained parameters and estimated barrier heights are presented in Table 2. The barrier heights of 3-AP depend on

Table 2 Observed and calculated energy levels of the NH_2 inversion vibration of different aminophenol isomers, together with parameters of the potential function and barrier heights. For *trans* 2-AP the energy levels were calculated by fitting the experimental data to the model potential function, constrained by the calculated B3LYP/cc-pVTZ potential energy profile. The energy levels and barrier heights of 4-AP and *trans* 2-AP, calculated from an *ab initio* potential alone, are also shown.

	$v_I=1$		$v_I=2$		$v_I=3$		$v_I=4$		Calculated barrier height, cm^{-1}	Potential function constants		
	Obs.	Calc.	Obs.	Calc.	Obs.	Calc.	Obs.	Calc.		B	ρ	v_0
From experimental data												
trans 3-AP	55	55	420	420	714	714	-	1099	452.6	0.6082	0.3546	744.2
cis 3-AP	50	50	422	422	717	717	-	1110	478.4	0.458	0.1914	1044.8
4-AP	-	36.1	467	467	711	711	1085[35]	1085	635.7	1.2756	0.9331	498.0
trans 2-AP	-	37.2	437	437	696	696	-	1071	568.4	0.8898	0.5326	638.8
From *ab initio* potential												
4-AP	-	25.9	467	478.1	711	700.3	1085[35]	1075.1	706.9	1.2966	0.8155	545.2
trans 2-AP	-	38.9	437	445.9	696	707.7	-	1086.4	576.8	0.9650	0.6225	597.7

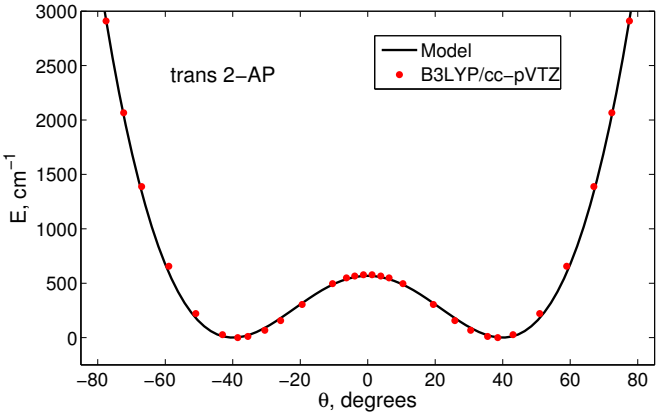

Fig. 6 NH_2 inversion (wagging) potential of *trans* 2-AP, obtained from fitting of experimentally observed transitions within the model of double-minimum harmonic well potential with a gaussian barrier (in black), constrained by potential energy profile calculated with B3LYP/cc-pVTZ method (shown with red dots). The observed 0-2 and 0-3 vibrational transitions of NH_2 inversion of *trans* 2-AP were used. θ is the angle between the plane of amino-group and phenyl ring.

the orientation of the OH group with respect to NH_2, and have the values of 453 and 478 cm^{-1} for the *trans* and *cis* conformers, respectively. We note that if the alternative assignments of 0-3 transitions with the frequencies of 698 and 700 cm^{-1} were used, the corresponding estimated barriers would change to 457 and 481 cm^{-1} and the corresponding theoretical 0-4 transitions would then appear at 1065 and 1073 cm^{-1}. A similar approach was used for the treatment of 4-AP. Since for 4-AP we only observed the 0-2 and 0-3 transitions, while at least three frequencies are required, we additionally used the 0-4 transition frequency obtained from dispersed fluorescence experiments[35]. The results for 4-AP are listed in Table 2.

Since, in contrast to 3-AP and 4-AP, for *trans* 2-AP only two transition frequencies associated with the NH_2 inversion motion are measured, a different approach to find the parameters B, ρ and v_0 was implemented. We first calculated the *ab initio* potential energy profile governing the NH_2 inversion motion by a relaxed potential energy scan with the B3LYP/cc-pVTZ method. Then, a trial potential function (Eq. 1) was optimized with the least squares method to best describe the calculated *ab initio* potential energy as well as the frequencies of the observed 0-2 and 0-3 experimental transitions. The optimized analytic potential function is presented in Fig. 6 together with *ab initio* calculations, and the corresponding potential parameters are listed in Table 2. The theoretical energy levels of *trans* 2-AP and 4-AP were also calculated from the *ab initio* potential alone (see Table 2), resulting in relatively good agreement between the calculated and observed transitions (deviations in frequency of 0-2, 0-3 and 0-4 transitions are close to 10 cm^{-1}). Overall, despite the relatively low computational cost of the B3LYP/cc-pVTZ method used for the calculation of the potential energy profile, the experimental data agree very well with the theoretical predictions.

4 Discussion

The comparison of our experimental data with the quantum chemical analysis shows that many structure-specific signatures of aminophenol in the far-IR are not well reproduced both within the harmonic approximation as well as the VPT2 treatment. When anharmonicity of the vibrational motion is large, which is the case for the NH_2 wagging motion, the second-order perturbation theory naturally fails at accurately calculating the frequencies and intensities of the corresponding vibrational transitions. However, for the weakly anharmonic modes, the theoretical frequencies can be obtained successfully with the VPT2 treatment providing better agreement with the experiment than their harmonic counterparts (see Fig. 4). If most of the vibrations of the molecule are weakly anharmonic, as in the case of semi-rigid molecules studied by Barone *et al.*[22], the VPT2 treatment gives computationally cheap and reliable results, sufficient for spectroscopic studies. The strongly anharmonic motions (large amplitude vibrations) can be treated separately (*e.g.* with the variational approach), but for large molecules with a large number of such vibrations, this treatment is computationally expensive and gets complicated by significant contributions from vibrational couplings. For the medium-sized aminophenol molecule, we were able to describe the strongly anharmonic NH_2 wagging motion with a double-minimum potential model and variational treatment, which provided a reliable assignment for the observed far-IR features, and enabled us to obtain the NH_2 inversion barrier values. The calculations of the vibrational energy levels from the *ab initio* potential fitted to the double-minimum model also provided the qualitative positions of the NH_2 wagging vibrational

transitions.

The height of the barrier to NH_2 inversion reflects the difference between the electron donating (by resonance) and electron withdrawing (by induction) abilities of the substituent group in aniline derivatives[33,46]. In this respect the higher electron density on the nitrogen atom of the amino group corresponds to a higher barrier to inversion (planarity). Aminophenol molecule represents the aniline derivative as well, with the hydroxyl OH group as a substituent. The differences between the obtained inversion barriers of the aminophenol isomers (see Table 2) and aniline molecule (526 cm^{-1}) are in good agreement with the resonant and inductive abilities of the OH group. As proposed by Kydd and Krueger[46], the observed variations in barrier height of substituted anilines can be explained by the differences between Hammett substituent constants σ_I and σ_R[47], which correspond to the inductive and resonant components of the overall substitutent constant σ. Among the previously studied substituents (F, Cl, Br, Me), the hydroxyl group has an intermediate value of inductive constant $\sigma_I = 0.28$. This suggests that the barrier to inversion in 3-AP has to be higher than in halosubstituted anilines, and lower than in methylaniline. The barrier height estimated from our experimental data for the *cis* conformer of 3-AP is 478 cm^{-1}, which agrees well with this statement. In contrast, the estimated value of the barrier of the *trans* conformer is 453 cm^{-1}, comparable to the values of halosubstituted anilines. This observation is indicative of slightly lower electron density on the nitrogen atom in the *trans* configuration, where the OH group is opposite to the NH_2 group. The simple linear relation between the barrier height and inductive substituent constant σ_I, suggested in Ref.[46], yields the value of 489.6 cm^{-1} for the barrier of 3-AP, which is close to the value we estimated for the *cis* 3-AP.

The resonant constant of the OH group has the value $\sigma_R = -0.40$, which is slightly higher than in the case of fluorine substitution ($\sigma_R = -0.35$, see Table 1.4 of Ref.[47]). In 4-AP, where the resonant interactions also play a role, the estimated barrier to inversion is 637 cm^{-1} (see Table 2), that is higher than, for instance, in the case of fluoroaniline[33] (600 cm^{-1}). This result is in agreement with the higher electron donating (resonance) ability of the OH group (and higher absolute value of σ_R). Again, the simple linear relation between the barrier height and the Hammett constants σ_I and σ_R[46] yields the value of 657 cm^{-1} for 4-AP, which is quite close to the experimental value. In the case of 2-AP, the experimental value of the barrier to inversion is 568 cm^{-1}, much higher than for 3-AP, as expected, but lower than for 4-AP. Indeed, in 2- (*ortho*-) substitutions not only resonance, but also hydrogen bonding and steric interactions play a role, thus lowering the barrier in 2-AP with respect to 4-AP.

5 Conclusions

The experimental conformer-specific far-IR spectra of three isomers of aminophenol in the range of 220-800 cm^{-1} showed a wealth of distinct absorption bands with different frequencies and intensities for each isomer. Despite the minor differences in the structure, the *trans* and *cis* conformers of 3-AP were well distinguished as well, mostly due to the variations in the frequencies of the NH_2 and OH torsional vibrations, and the CH o.p. wagging. The anharmonic VPT2 approach has enabled us to successfully reproduce the frequencies of weakly anharmonic vibrations of aminophenol in the studied range, such as ring i.p. and o.p. deformations, C-O and C-N o.p. bending, and C-H o.p. wagging. The best accuracy was obtained by the hybrid B3LYP functional with a double-zeta basis set of moderate quality. However, the strongly anharmonic vibrations such as NH_2 wagging (inversion) were problematic for conventional DFT frequency calculations. To treat these modes, we applied a model of double-minimum harmonic well potential with a Gaussian barrier. Using that model, the values of the NH_2 inversion barrier and the parameters of the double well potential were obtained. The differences between the obtained inversion barriers of the aminophenol isomers and aniline molecule are in good agreement with the electron withdrawing (by induction) and donating (by resonance) abilities of the substituent OH group. Moreover, it was found that the model double-minimum potential obtained from the B3LYP/cc-pVTZ potential energy surface scan is reliable to qualitatively reproduce the frequencies of the observed NH_2 inversion transitions.

In spite of the remaining difficulties in the theoretical treatment of far-IR and THz spectra, the structural analysis based on the vibrational signatures in this spectral region is very promising. The development of efficient, generally applicable theoretical methods is therefore highly important. For instance, the explicit variational treatment of strongly anharmonic motions in the case of large molecules is much more challenging than in the case of aminophenol. One of the encouraging alternatives are *ab initio* molecular dynamics simulations[10,11,48], which are capable of naturally taking into account all anharmonic effects and conformational dynamics even for large and floppy biomolecular systems. We anticipate that the data obtained in this study will serve as a benchmark for the development of new theoretical methods tailor-made for far-IR action spectroscopy.

6 Acknowledgments

We acknowledge the Swedish Research Council (VR), the Knut and Alice Wallenberg Foundation (Sweden) and the Dutch Foundation for Fundamental Research on Matter (FOM) for financial support. This work was also partly supported through the CALIPSO project of the European Union. The authors highly appreciate the skilful assistance of the staff at the FELIX laboratory and acknowledge SURFsara (www.surfsara.nl) for providing computational resources at the Lisa Computing Cluster.

References

1 H. Mantsch and D. Naumann, *J. Mol. Struct.*, 2010, **964**, 1–4.
2 G. Acbas, K. A. Niessen, E. H. Snell and A. Markelz, *Nat. Commun.*, 2014, **5**, 3076.
3 D. F. Plusquellic, K. Siegrist, E. J. Heilweil and O. Esenturk, *ChemPhysChem*, 2007, **8**, 2412 – 2431.
4 R. J. Falconer and A. G. Markelz, *J. Infrared, Millimeter, Terahertz Waves*, 2012, **33**, 973–988.
5 C. Soto, *Nature Reviews Neuroscience*, 2003, **4**, 49–60.
6 Y. S. Eisele, C. Monteiro, C. Fearns, S. E. Encalada, R. L. Wise-

man, E. T. Powers and J. W. Kelly, *Nature Reviews Drug Discovery*, 2015, 759–780.
7 K. Itoh and T. Shimanouchi, *Biopolymers*, 1967, **5**, 921–930.
8 K. Itoh, T. Shimanouchi and M. Oya, *Biopolymers*, 1969, **7**, 649–658.
9 V. C. Nibali and M. Havenith, *Journal of the American Chemical Society*, 2014, **136**, 12800–12807.
10 S. Jaeqx, J. Oomens, A. Cimas, M.-P. Gaigeot and A. M. Rijs, *Angew. Chem. Int. Ed.*, 2014, **53**, 3663 –3666.
11 J. Mahe, S. Jaeqx, A. M. Rijs and M.-P. Gaigeot, *Phys. Chem. Chem. Phys.*, 2015, **17**, 25905–25914.
12 *Gas-Phase IR Spectroscopy and Structure of Biological Molecules*, ed. A. M. Rijs and J. Oomens, Top. Curr. Chem., 2015, vol. 364, pp. 1–406, and references therein.
13 A. M. Rijs, M. Kabelac, A. Abo-Riziq, P. Hobza and M. S. de Vries, *ChemPhysChem*, 2011, **12**, 1816–1821.
14 N. S. Nagornova, T. R. Rizzo and O. V. Boyarkin, *Journal of the American Chemical Society*, 2010, **132**, 4040–4041.
15 K. Joshi, D. Semrouni, G. Ohanessian and C. Clavaguera, *The Journal of Physical Chemistry B*, 2012, **116**, 483–490.
16 J. A. Stearns, C. Seaiby, O. V. Boyarkin and T. R. Rizzo, *Phys. Chem. Chem. Phys.*, 2009, **11**, 125–132.
17 M. Rossi, V. Blum, P. Kupser, G. von Helden, F. Bierau, K. Pagel, G. Meijer and M. Scheffler, *J. Phys. Chem. Lett.*, 2010, **1**, 3465–3470.
18 K.-K. Lee, K.-H. Park, J.-H. Choi, J.-H. Ha, S.-J. Jeon and M. Cho, *The Journal of Physical Chemistry A*, 2010, **114**, 2757–2767.
19 A. M. Rijs and J. Oomens, *IR Spectroscopic Techniques to Study Isolated Biomolecules*, Top. Curr. Chem., 2015, vol. 364, pp. 1–42.
20 R. D. Amos, N. C. Handy, W. H. Green, D. Jayatilaka, A. Willetts and P. Palmieri, *J. Chem. Phys.*, 1991, **95**, 8323.
21 V. Barone, *J. Chem. Phys.*, 2005, **122**, 014108.
22 V. Barone, M. Biczysko and J. Bloino, *Phys. Chem. Chem. Phys.*, 2014, **16**, 1759–1787.
23 M. J. Frisch, G. W. Trucks, H. B. Schlegel, G. E. Scuseria, M. A. Robb, J. R. Cheeseman, G. Scalmani, V. Barone, B. Mennucci, G. A. Petersson, H. Nakatsuji, M. Caricato, X. Li, H. P. Hratchian, A. F. Izmaylov, J. Bloino, G. Zheng, J. L. Sonnenberg, M. Hada, M. Ehara, K. Toyota, R. Fukuda, J. Hasegawa, M. Ishida, T. Nakajima, Y. Honda, O. Kitao, H. Nakai, T. Vreven, J. A. Montgomery, Jr., J. E. Peralta, F. Ogliaro, M. Bearpark, J. J. Heyd, E. Brothers, K. N. Kudin, V. N. Staroverov, R. Kobayashi, J. Normand, K. Raghavachari, A. Rendell, J. C. Burant, S. S. Iyengar, J. Tomasi, M. Cossi, N. Rega, J. M. Millam, M. Klene, J. E. Knox, J. B. Cross, V. Bakken, C. Adamo, J. Jaramillo, R. Gomperts, R. E. Stratmann, O. Yazyev, A. J. Austin, R. Cammi, C. Pomelli, J. W. Ochterski, R. L. Martin, K. Morokuma, V. G. Zakrzewski, G. A. Voth, P. Salvador, J. J. Dannenberg, S. Dapprich, A. D. Daniels, Ö. Farkas, J. B. Foresman, J. V. Ortiz, J. Cioslowski and D. J. Fox, *Gaussian 09 Revision D.01*, Gaussian Inc. Wallingford CT 2009.
24 A. D. Becke, *J. Chem. Phys.*, 1993, **98**, 5648–5652.
25 J. Coon, N. Naugle and R. McKenzie, *Journal of Molecular Spectroscopy*, 1966, **20**, 107 – 129.
26 I. Lopez-Tocon, R. G. D. Valle, M. Becucci, E. Castellucci and J. C. Otero, *Chem. Phys. Lett.*, 2000, **327**, 45 – 53.
27 M. H. Jamroz, *Spectrochim. Acta, Part A*, 2013, **114**, 220–230.
28 M. C. Capello, M. Broquier and S.-I. Ishiuchi et al., *J. Phys. Chem. A*, 2014, **118**, 2056–2062.
29 W. Y. Sohn, M. Kim, S.-S. Kim, Y. D. Park and H. Kang, *Phys. Chem. Chem. Phys.*, 2011, **13**, 7037–7042.
30 H. Mori, H. Kugisaki, Y. Inokuchi, N. Nishi, E. Miyoshi, K. Sakota, K. Ohashi and H. Sekiya, *Chem. Phys.*, 2002, **277**, 105 – 115.
31 T. W. Robinson and H. G. K. et al., *J. Phys. Chem. A*, 2004, **108**, 4420–4427.
32 *Vibrational Spectra of Benzene Derivatives*, ed. G. Varsanyi, Academic Press, 1969.
33 R. A. Kydd and P. J. Krueger, *J. Chem. Phys.*, 1978, **69(2)**, 827.
34 R. A. Kydd and P. J. Krueger, *Chem. Phys. Letters*, 1977, **49(3)**, 539.
35 S. Wategaonkar and S. Doraiswamy, *J. Chem. Phys.*, 1996, **105**, 1786.
36 G. N. Patwari, S. Doraiswamy and S. Wategaonkar, *Phys. Chem. Chem. Phys.*, 1999, **1**, 2279–2286.
37 V. Barone, P. Cimino and E. Stendardo, *J. Chem. Theory Comput.*, 2008, **4**, 751–764.
38 *Double and triple-zeta basis sets of SNS and N07 families are available online*, http://dreamslab.sns.it, (accessed February 1, 2015).
39 K. L. Schuchardt, B. T. Didier, T. Elsethagen, L. Sun, V. Gurumoorthi, J. Chase, J. Li and T. L. Windus, *J. Chem. Inf. Model.*, 2007, **47**, 1045–1052.
40 C. Unterberg, A. Gerlach, A. Jansen and M. Gerhards, *Chem. Phys.*, 2004, **304**, 237 – 244.
41 H. Mori, H. Kugisaki, Y. Inokuchi, N. Nishi, E. Miyoshi, K. Sakota, K. Ohashi and H. Sekiya, *Chem. Phys.*, 2002, **277**, 105 – 115.
42 *NIST Mass Spec Data Center, S.E. Stein, director, "Infrared Spectra" in NIST Chemistry WebBook, NIST Standard Reference Database Number 69*, http://webbook.nist.gov, (retrieved May 21, 2015).
43 M. Biczysko, P. Panek, G. Scalmani, J. Bloino and V. Barone, *J. Chem. Theory Comput.*, 2010, **6**, 2115–2125.
44 A. D. Boese, W. Klopper and J. M. L. Martin, *Int. J. Quantum Chem.*, 2005, **104**, 830–845.
45 M. W. D. Hanson-Heine, M. W. George and N. A. Besley, *The Journal of Physical Chemistry A*, 2012, **116**, 4417–4425.
46 R. A. Kydd and P. J. Krueger, *The Journal of Chemical Physics*, 1980, **72**, 280–283.
47 *Advances in Linear Free Energy Relationships*, ed. N. B. Chapman and J. Shorter, Springer US, 1972.
48 M.-P. Gaigeot, *Phys. Chem. Chem. Phys.*, 2010, **12**, 3336–3359.